Talanta 300 (2026) 129253

Contents lists available at ScienceDirect

Talanta

journal homepage: www.elsevier.com/locate/talanta

Enhanced amperometric tyramine sensing via tyrosinase entrapment in polyethylene glycol-modified methacrylate microgels

Juan Pablo Hervás-Pérez [a], Laura Martín-Carbajo [a], Sergio Izcara [b,c], Marta Sánchez-Paniagua [a,*]

[a] Department of Chemistry in Pharmaceutical Sciences, Faculty of Pharmacy, Complutense University of Madrid, 28040, Madrid, Spain
[b] Faculty of Health Sciences – HM Hospitals, University Camilo José Cela, Urb. Villafranca del Castillo, 49., Villanueva de la Cañada, 28692, Madrid, Spain
[c] Instituto de Investigación Sanitaria HM Hospitales, 28015, Madrid, Spain

ARTICLE INFO

Keywords:
Electrochemical biosensor
Microgel
Tyrosinase
Tyramine
Food control

ABSTRACT

A highly sensitive and selective tyrosinase-based electrochemical biosensor for tyramine detection in complex food matrices was developed using polyethylene glycol-poly(methacrylic acid) microgels (PEG-pMAA) as enzyme immobilization matrix. The morphology and particle size of the obtained PPO-PEG-pMAA microgel were studied by SEM and particle analyzer system, obtained polydisperse microgels in the range of 2–18 μm with a 6.2 μm of average particle size. Incorporation of PEG during microgel polymerization provided a favorable microenvironment for enzyme activity, resulting in a 22 % higher amperometric response toward tyramine compared to microgels without PEG (PPO-pMAA), without compromising reproducibility (RSD ≤6.1 %). The PPO-PEG-pMAA biosensor's performance was optimized in terms of cross-linking degree, PEG %, pH, potential, temperature, enzyme loading and microgel deposition. A complete enzyme entrapment at pH 6 in microgel synthesis with a cross-linking ratio of 2 %, which balanced enzyme retention and substrate accessibility is obtained. Under optimal conditions, the device exhibited a wide linear range ($2.0 \times 10^{-7} - 4.7 \times 10^{-5}$ M), low detection limit (45 nM) and rapid amperometric responses (50 s). The freeze-dried microgels were stable 9 months and the microgel-based biosensor retained 95–100 % of its initial response during 35 days of storage, confirming excellent stability. Interference studies showed negligible effects from the most abundant acids and amino acids present in cheese, highlighting the device's selectivity. Application to cheese samples, including Brie and Gouda, yielded recoveries between 97.6 and 105.6 %, and allowed monitoring of tyramine accumulation during storage, demonstrating the biosensor's reliability and suitability as a rapid and practical tool for tyramine screening in complex food matrices.

1. Introduction

Tyramine is a naturally occurring biogenic amine produced via the enzymatic decarboxylation of the amino acid tyrosine. It is frequently present in fermented and aged food products such as cheeses, cured meats, fish derivatives, wines, and beers [1,2]. Although it plays a physiological role in modulating blood pressure and neurotransmission, excessive tyramine intake can cause hypertensive crises, headaches, and cardiovascular disorders, particularly in individuals treated with monoamine oxidase inhibitors (MAOIs) [3]. Toxicological assessments and recent reviews indicate that healthy individuals tolerate relatively high dietary tyramine loads (no-observed-adverse-effect level, NOAEL, ~600 mg per meal), whereas individuals treated with classical monoamine-oxidase inhibitors (MAOIs) may experience hypertensive reactions at intakes as low as a few milligrams per meal (classically cited values ≈ 6 mg), underscoring the clinical relevance of sensitive tyramine monitoring in foodstuffs [2,3]. Consequently, reliable detection and quantification of tyramine in food matrices is essential to ensure food safety and compliance with regulatory standards [1].

Conventional analytical methodologies for tyramine quantification predominantly rely on chromatographic techniques such as high-performance liquid chromatography (HPLC), ultra-performance liquid chromatography (UPLC), and gas or liquid chromatography coupled with mass spectrometry (GC-MS or LC-MS/MS) [4,5]. These platforms

* Corresponding author.
E-mail addresses: jphervas@ucm.es (J.P. Hervás-Pérez), lauramartin@ucm.es (L. Martín-Carbajo), sergio.izcara@ucjc.edu (S. Izcara), martasan@ucm.es (M. Sánchez-Paniagua).

https://doi.org/10.1016/j.talanta.2025.129253
Received 11 November 2025; Received in revised form 4 December 2025; Accepted 10 December 2025
Available online 15 December 2025

offer outstanding sensitivity and selectivity; however, it requires labor-intensive sample preparation, high operational costs, and the need for specialized personnel and instrumentation factors that hinder their applicability in routine or on-site analysis. In this sense, electrochemical biosensors have emerged as promising alternatives, offering high sensitivity, operational simplicity, portability, and cost-effectiveness [6]. Their ability to deliver rapid and reliable results with minimal sample preparation makes them particularly attractive for decentralized food safety monitoring and POC applications. As example, a gold nanoparticle doped poly (8-anilino-1-naphthalene sulphonic acid) based-tyrosinase biosensor was used for tyramine detection in dairy products and fermented drinks, exhibited a linear response from 10 to 120 μM with a detection limit of 0.71 μM [7]. More recently, Kocoglu et al. developed a biosensor based on carbon nanofibers, an ionic liquid, and poly (glutamic acid) to immobilize tyrosinase for the selective determination of tyramine. The device exhibited a wide linear range (0.2–48 μM), low detection limit (0.091 μM) and was applied to tyramine detection in malt beverages and pickle juice [8]. These developments demonstrate the rapid progress of enzyme-based electrochemical biosensors toward achieving high analytical sensitivity, selectivity, and stability for tyramine detection in complex matrices.

A major challenge in the design of enzyme-based biosensors lies in achieving stable and active immobilization of the biorecognition element. An effective immobilization strategy must prevent enzyme leaching, preserve catalytic activity, and ensure unhindered diffusion of substrates and products [9,10]. Among the available immobilization strategies—physical adsorption, covalent bonding, entrapment, or encapsulation—the use of polymeric microgels has established as a promising route. Microgels are crosslinked polymeric networks in the micro-to submicrometer range that provide a hydrated three-dimensional matrix ideal for preserving enzyme conformation and activity [11,12]. Their tunable porosity, chemical versatility, and large surface-to-volume ratio facilitate high enzyme loading and efficient mass transport. Moreover, they can be engineered to respond to environmental stimuli (pH, temperature, ionic strength), enabling dynamic regulation of permeability and catalytic performance [12,13].

Recent studies have demonstrated that the immobilization of enzymes within microgel networks substantially enhances operational stability and reusability compared to free enzymes [10]. Some authors reviewed the application of hydrogel-based enzyme systems, highlighting their superior structural compatibility and long-term performance [14,15]. Silva et al. emphasized the role of responsive microgel assemblies in biosensing and biocatalysis, showing that structural tunability and interfacial interactions directly influence catalytic efficiency [12]. Furthermore, hierarchical and porous supports based on methacrylate derivatives have been successfully employed for enzyme immobilization in food and environmental biosensors, confirming the adaptability and robustness of such systems [12,13,16].

In this context, methacrylate-based polymers—notably poly (methacrylic acid, pMAA) and related copolymers—represent one of the most versatile materials for constructing microgel immobilization matrices [10,17,18]. Methacrylate networks exhibit excellent mechanical and chemical stability under varying pH and ionic conditions, ensuring prolonged operational lifetimes in real food analysis environments [17]. Furthermore, the compatibility of methacrylate's with photopolymerization and microfabrication enables their integration into miniaturized transducers and lab-on-chip systems. Among these, poly (acrylic acid) (PAA) and pMAA stand out due to their pH-responsiveness and biocompatibility. The ionization of carboxylic groups induces swelling–deswelling transitions that modulate mass transport and substrate accessibility within the network [19,20]. This property has been successfully exploited for biosensors operating in physiological or food-related media, where pH fluctuations can influence analytical response. Notably, Hervás-Pérez et al. demonstrated that pMAA-based microparticles with immobilized glucose oxidase exhibited strong relationships between monomer concentration, crosslinker ratio, and polymerization conditions, achieving enhanced enzyme loading, stability, and sensitivity [16]. PEG has also been incorporated into the methacrylate microgel formulation to act both as a hydrophilic modifier—enhancing network water retention, local hydration and substrate diffusion that preserve enzyme conformation—and as a polymerization stabilizer that improves microgel homogeneity and reproducibility of pore architecture; PEG-mediated stabilization of enzymes and PEG-controlled hydrogel properties have been documented in recent experimental and review studies [21–23].

Such findings underscore the potential of methacrylate microgels as robust immobilization matrices for enzymatic biosensors targeting analytes like tyramine in complex food matrices.

This work proposes the development of a highly sensitive and stable biosensor for the detection of tyramine in food matrices. The device is based on the use of poly(methacrylate) microgels as the immobilization matrix. During the microgel synthesis, polyethylene glycol (PEG) was incorporated as a stabilizing and hydrophilic modifier, improving polymerization control and enhancing the biocompatibility of the support. This hybrid polymeric network provides a more favorable microenvironment for enzyme activity, resulting in increased immobilization efficiency and improved electrochemical detection performance toward tyramine. These performance metrics not only surpass those of previously reported tyramine biosensors employing conventional enzyme immobilization strategies but also demonstrate the significant analytical advantages derived from the entrapment of tyrosinase within PEG-modified methacrylate microgels. Under optimized assay conditions, the biosensor exhibited a linear detection range from $2.0 \times 10^{-7} - 4.7 \times 10^{-5}$ M, a LOD of 4.5×10^{-8} M, and LOQ of 1.2×10^{-7} M. Building upon these considerations, this study aims to develop and characterize a highly sensitive electrochemical biosensor based on this microgel architecture, emphasizing its improved immobilization efficiency, catalytic performance, and operational stability. Overall, the proposed platform provides a promising pathway toward rapid, reliable, and cost-effective monitoring of biogenic amines in complex food matrices.

2. Material and methods

2.1. Reagents

Polyphenol oxidase (PPO, EC 1.14.18.1; tyrosinase from mushrooms, 1530 U/mg), tyramine, tyrosine, phenylalanine, glutamic acid, histamine, putrescine, methacrylic acid (MAA), N,N'-methylenebisacrylamide (BIS), polyethylene glicol 4000 (PEG), potassium hexacyanoferrate (II) ($Fe(CN)_6^{4-}$) and potassium hexacyanoferrate(III) ($Fe(CN)_6^{3-}$) were purchased from Sigma-Aldrich (St. Louis, MO, USA). Ammonium persulfate (PSA), N,N,N′,N' tetramethylethylendiamine (TEMED) and the surfactant Span 80 were obtained from Fluka (Buchs, Switzerland). Sodium dihydrogen phosphate, disodium hydrogen phosphate, sodium acetate, calcium chloride, magnesium chloride, and sodium nitrate were supplied from Panreac (Barcelona, Spain). The dialysis membrane (12,000–14,000 MWCO) was purchased from Spectrum Medical Industries. All aqueous solutions were prepared using ultrapure water obtained from a Milli-Q purification system (Millipore, Milford, MA, USA).

2.2. Instrumentation and measurements

The morphology of the synthesized microgels was examined by scanning electron microscopy (SEM) using a JEOL JSM-6400 microscope (JEOL, Japan) operated at an accelerating voltage of 20 kV and a magnification of 5000 × . Samples were dried on copper grids, and surface replicas were prepared by gold sputtering using a Balzers SCD-004 sputter coater. The particle size measurements, in the range of 2–150 μm, were determined using a Galai CIS-1 particle analyzer system, which combines a laser-based analyzer and a video-based shape analyzer. The laser-based analyzer evaluates the particles diameter by

the time it takes a particle to cross a laser beam. The pH of buffer solutions was adjusted using a Mettler Toledo MP230 pH meter.

Electrochemical measurements were carried out on a μ-Autolab PGSTAT12 potentiostat (EcoChemie, The Netherlands) controlled by GPES 4.9 software, employing a conventional three-electrode cell configuration. A modified glassy carbon working electrode (3 mm diameter) was used, together with a platinum wire as the counter electrode and an Ag/AgCl (3 M KCl) reference electrode. All amperometric measurements were performed in a thermostated electrochemical cell connected to a Julabo circulating thermostat (range: 5–200 °C). Amperometric measurements were performed by applying a detection potential of −0.05 V, followed by the addition of a tyramine solution after baseline stabilization. The results were based on the difference between the steady-state and background currents. Calibration curves were obtained by recording the steady-state current response after successive additions of substrate solution into 10 mL of stirred phosphate buffer (pH 6.0). Sensitivity was determined from the slope of the calibration plot, whereas the limit of detection (LOD) was calculated as the substrate concentration corresponding to a signal-to-noise ratio of 3. The response time was defined as the time required to reach 95 % of the steady-state current after substrate addition. Electrochemical impedance spectroscopy (EIS) experiments were conducted at the open-circuit potential (OCP) using a sinusoidal perturbation of 5 mV (peak-to-peak) over a frequency range from 10^4 to 0.1 Hz, with 5 mM $Fe(CN)_6^{3-/4-}$ redox probe in 0.1 M KCl. The impedance data were represented as Nyquist plots and fitted to a Randles equivalent circuit to extract the charge transfer resistance (R_{ct}).

To evaluate the catalytic efficiency of the enzyme immobilization system, a comparative spectrophotometric study was performed by measuring the absorbance of the reaction products at 380 nm using a Genesys 10 spectrophotometer (Thermo Scientific, Spain).

2.3. Synthesis of PPO based-PEG-pMAA microgels

PEG-poly(methacrylic acid) (pMAA) microgels were synthesized using the water/oil (W/O) concentrated emulsions following a previously reported protocol [16], with slight modifications. The dispersed aqueous phase consisting of MAA (1.19 M), BIS (variable concentration), ammonium persulfate (10.96 mM) and TEMED (84 mM). The continuous oil phase consists of 3.3 M of dodecane and 0.58 M of Span 80). The cross-linking density of the microparticles was modulated by the ratio between the weights of the cross-linker and the monomer (η). The cross-linker content was adjusted between 1.0 % and 3.5 %. The immobilization of polyphenol oxidase (PPO, 3000 U/mL) was achieved by incorporating the enzyme into the aqueous phase of the concentrated emulsion prior to polymerization. Polyethylene glycol 5 % (PEG 4000) was also added to the aqueous phase as a stabilizing and crowding agent to improve the retention of enzymatic activity during polymerization and to enhance the microenvironmental hydrophilicity of the gel matrix. PEG acts as a protective osmolyte, reducing enzyme denaturation at the water–oil interface and limiting the diffusion of free radicals toward the enzyme during polymerization, thereby preserving its native conformation and catalytic performance [24]. After isolation of the microparticles by centrifugation (7500 rpm, 20 min, 5 °C) and washing with water, the resulting supernatant was collected and stored for later determination of the enzymatic activity of the synthesized microparticles.

The polymerization process was carried out for 90 min under controlled temperature conditions (<25 °C) to preserve the catalytic integrity of the enzyme. This reaction time was selected based on previous studies demonstrating a monomer conversion degree of approximately 99 % under similar conditions [16]. Considering that polymerization temperature depends on the concentration of the initiator, a persulfate concentration of 10.96 mM was used to prevent thermal inactivation of the enzyme, as previously was reported for analogous enzymatic systems [16].

2.4. Preparation of the PPO-PEG-pMAA biosensor

The working electrode surface (3 mm diameter) was mechanically polished using a 0.05 μm alumina slurry to ensure a smooth and reproducible finish. After polishing, residual abrasive particles were removed by sequential ultrasonic cleaning in ethanol and distilled water. A precisely weighed amount of microgel particles was then deposited onto the electrode surface and secured with a dialysis membrane to ensure stable immobilization. The modified electrode was subsequently rinsed with phosphate buffer, immersed in PBS, and held at −0.05 V until the background current reached a stable baseline.

2.5. Real sample preparation

Cheese samples were obtained from local supermarkets. Sample preparation was carried out following a previously reported protocol [29]. Briefly, 1.0 g of brie or gouda cheese was accurately weighed and homogenized with 2 mL of 0.1 M phosphate buffer solution (PBS, pH 6.0). The mixture was vortexed for 1 min to ensure dispersion, followed by ultrasonic extraction in a water bath for 10 min to enhance analyte release. The resulting suspension was centrifuged at 3000 rpm for 10 min, and the supernatant was carefully collected. This extraction step was repeated twice under identical conditions, and the combined supernatants were stored at −20 °C until analysis. For electrochemical assays, 100 μL of the cheese extract was diluted in 10 mL of PBS within the electrochemical cell. The amperometry response was recorded under optimized conditions, and the tyramine concentration was quantified from the corresponding calibration curve. All measurements were performed in triplicate to ensure reproducibility.

3. Results and discussion

3.1. Characterization of the microparticles

The scanning electron micrographs (SEM) of PEG-pMAA microgels, both unloaded and PPO-loaded, reveal spherical and polydisperse microparticles (Fig. 1a and b). Particle size distribution analysis performed using a Particle-Size Analyzer System showed polydisperse microparticles with diameters ranging from 2 to 18 μm (Fig. 2a and b). Similar morphological characteristics have been reported for other methacrylate-based microgel systems [25,26]. The average particle size of the PPO-PEG-pMAA microgels was 6.2 μm, which was comparable to that of the empty PEG-pMAA microgels (5.7 μm) prepared under identical cross-linking conditions (η = 2 %). This similarity in particle size suggests that enzyme incorporation did not significantly influence the polymerization process or compromise the structural integrity of the resulting microgels.

The polydispersity of the microgels was determined from the cumulative particle size distribution and expressed as the polydispersity coefficient calculated using the D90/D10 ratio [27]. The PPO–PEG–pMAA microgels exhibited percentile values of P10 = 2 μm, P50 = 4 μm, and P90 = 12 μm, revealing a broad particle size range and substantial heterogeneity within the sample. The resulting D90/D10 ratio of 6 denotes a wide particle size distribution, clearly indicating that the microgels are highly polydisperse. A comparable D90/D10 value was also obtained for the PEG–pMAA microgels, confirming similarly broad size distributions.

pMAA-based microgels containing immobilized enzyme but without PEG exhibited a slightly smaller average particle size (5.1 μm) and a narrower size distribution (Fig. 1c and 2c). This observation indicates that the incorporation of PEG slightly increases the polydispersity of the synthesized particles, likely due to the formation of looser and more porous polymeric networks, as previously reported by other authors [22,23].

Table S1 summarizes the mean particle sizes obtained for microgels synthesized with varying crosslinking degrees (η, %) and different PEG

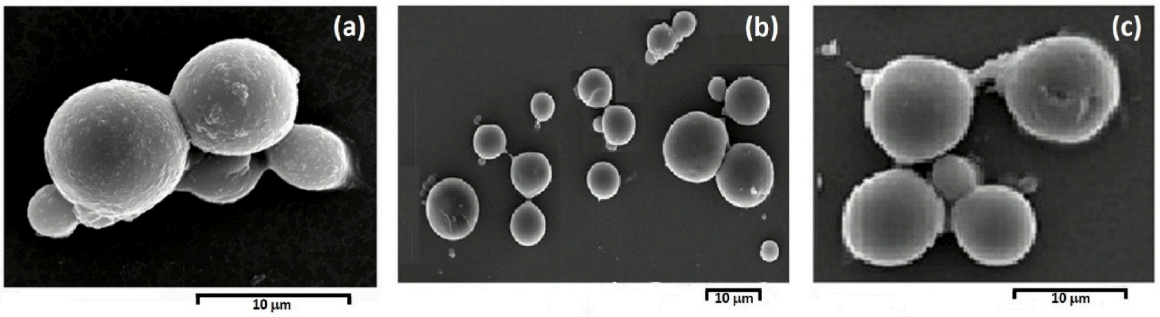

Fig. 1. SEM micrograph of freeze-dried PEG-pMAA (a), PPO-PEG-pMAA (b) and PPO-pMAA (c) microparticles.

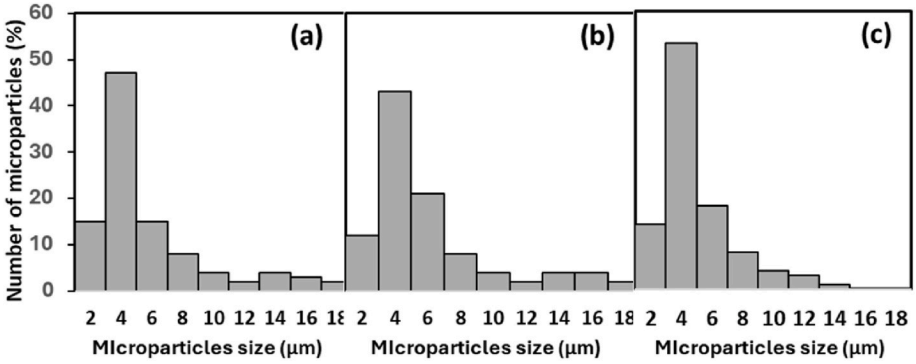

Fig. 2. Size distribution of PEG-pMAA (a), PPO-PEG-pMAA (b) and PPO-pMAA (c) microparticles dispersed in buffer (η = 2 %).

contents. The influence of these parameters on particle size and polydispersity coefficient will be discussed in the following sections.

3.2. Optimization of microparticle synthesis parameters

The influence of synthesis parameters, including the degree of microparticle crosslinking, PEG content, and pH in the polymerization synthesis, on the efficiency of tyrosinase immobilization was evaluated.

3.2.1. Effect of the cross-linking content

The cross-linking content (η) was crucial in tailoring the pore architecture of methacrylate-based microgels, directly impacting the entrapment efficiency of PPO and the overall biosensor performance. In this study, the monomer concentration was fixed at 1.59 M (previously identified as optimal for methacrylate microgel synthesis [16]), while the bis-acrylamide content was varied to modulate cross-linking. The enzyme concentration was maintained at 2000 U/mL, with 2 % of PEG included in the polymerization process. A deposition of 2 mg of microgel particles was applied onto the electrode surface. As shown in Table 1, the highest amperometric response toward 0.5 mM tyramine (−0.1 V, pH 6.0, 25 °C) was achieved at a cross-linking ratio of 2.0 %. Microgels with lower cross-linking degrees exhibited excessively large pores, resulting in partial enzyme leaching and a significant decrease in the maximum current density (J_{max}). This was corroborated by detectable enzymatic activity in the supernatant following microgel synthesis. In contrast, higher cross-linking levels led to diminished current responses, attributed to the restricted diffusion within the denser polymer matrix, which hindered substrate accessibility and delayed product release. This phenomenon was further evidenced by an increase in biosensor response time, confirming the diffusional constraints imposed by excessive cross-linking (6 s for

η = 2% and 15 s for **η = 3%**).

The PPO–PEG–pMAA microgels with different crosslinker contents (η, %) and characterized in terms of average particle size and polydispersity (Table S1). The results reveal that increasing the crosslinker content from 1.5 % to 3.0 % leads to a gradual decrease in the average particle size, from 6.5 µm to 5.4 µm, indicating that higher crosslinking restricts particle growth. Concurrently, the D90/D10 ratio decreases from 6.2 to 5.3, suggesting a slight narrowing of the particle size distribution and a trend toward more uniform particles at higher crosslinker levels.

All these findings underscore the importance of fine-tuning the cross-linking ratio to balance enzyme retention and substrate-product diffusion, thereby optimizing biosensor sensitivity and response kinetics. The 2.0 % cross-linking condition emerges as the optimal compromise, offering robust enzyme immobilization without compromising analyte accessibility.

Table 1
Analytical properties of PPO-PEG-pMAA biosensors as a function of cross-linking degree or PEG content.

Analytical parameters	Cross-linking content (η, %)[a]				PEG content (%)[b]			
	1.5	2.0	2.5	3.0	0	2	5	10
J_{max} (µA/cm^2)	125.6	267.4	243.2	187.5	222.8	267.4	302.4	304.5
Sensitivity (mA/Mcm^2)	1.94×10^3	3.65×10^3	3.45×10^3	2.66×10^3	3.42×10^3	3.65×10^3	3.83×10^3	3.80×10^3

[a] PEG 2 %.
[b] η = 2 %.

3.2.2. Effect of the polyethylene glycol content

Once the optical cross-linking degree was established, the influence of PEG content (2–10 %) was evaluated using PEG-free pMAA microparticles as the reference system. When comparing the electrochemical response toward 0.5 mM tyramine obtained with biosensors fabricated with pMAA or PEG-pMAA microgels, maintaining a constant cross-linking degree (η = 2 %), a 22 % increase in amperometry signal was observed with the addition of 2 % PEG (Table 1). As discussed in Section 3.1, the incorporation of PEG during polymerization leads to microgels with higher polydispersity; however, this variation did not compromise reproducibility, as reflected by the low inter-electrode RSD values (n = 5) of 5.7 % for PEG-free and 6.1 % for PEG-containing microparticles. This enhancement confirms the beneficial role of PEG incorporation in improving the electrochemical performance of the resulting microgels. Notably, the maximum signal intensity was obtained for microgels synthesized with 5 % PEG (J_{max} = 302.4 μA/cm^2), with no additional enhancement in electrochemical activity at 10 %. Therefore, 5 % of PEG was selected as optimum content. No significant changes in average particle size or D90/D10 were observed in microgel without or with different percentage of PEG (Table S1) indicating that PEG mainly modulates the microenvironment of the microgels rather than their overall size or size distribution.

To assess the influence of PEG on the PPO immobilization process, two complementary analyses were conducted. First, the entrapment efficiency was determined by measuring the enzymatic activity remaining in the supernatant after microgel synthesis, enabling verification of whether PPO was fully incorporated into the particles. Second, the retention of enzymatic activity was evaluated by comparing the activity of PPO immobilized in microgels with that of the free enzyme. Both studies were monitored spectrophotometrically at 380 nm by following the formation of o-quinones upon addition of tyramine (0.5 mM). This approach allowed us to assess the extent to which the catalytic functionality of PPO is preserved in pMAA and PEG-pMAA microgels (η = 2 %, PEG content = 1 %, synthesis pH = 6). As summarized in Table S2, PEG-pMAA microgels exhibited no detectable enzymatic activity in the supernatant, indicating complete enzyme entrapment. In contrast, pMAA microgels showed approximately 20 % PPO activity in the supernatant, confirming partial enzyme loss during synthesis. The retention of enzymatic activity after immobilization was evaluated by preparing dispersions of the microparticles in PBS (0.1 M, pH 6.0) and monitoring o-quinone formation at 380 nm. The resulting activities were compared with those of a free-enzyme solution containing the same amount of PPO. A 22 % decrease in enzymatic activity was observed for PPO immobilized in pMAA microgels relative to the free enzyme, whereas this loss decreased to 15 % when PEG was incorporated during synthesis (Table S2). This enhanced retention is attributed to the hydrophilic and flexible nature of PEG chains, which generate a more hydrated and less rigid microenvironment around the enzyme, thereby reducing conformational restrictions. Notably, other polymer-based immobilization systems report substantially higher activity losses, such as 26 % for acrylamide matrices [28] and up to 40 % for 1-vinyl-3--ethylimidazolium bromide-based polymers [29]. All these findings underscore the effectiveness of PEG-pMAA microgels as a promising immobilization platform for PPO.

3.2.3. pH of the synthesis medium

The influence of the pH in the polymerization process on the immobilization efficiency of PPO within PEG-pMAA microgel matrix was investigated. pMAA is a well-known pH-responsive polymer, whose pendant carboxylic groups have a pKa of approximately 5.5. Above this value, deprotonation of the carboxyl moieties imparts a net negative charge to the polymer backbone, inducing electrostatic repulsion among polymer chains and resulting in microgel swelling. Conversely, below the pKa, the carboxyl groups are predominantly protonated, leading to charge neutralization and a collapsed, compact microgel structure [30]. Tyrosinase, with an isoelectric point (pI) of 4.2, remains negatively charged throughout the pH range investigated. Therefore, electrostatic interactions between the enzyme and the PMAA network are expected to strongly depend on the ionization degree of the polymer.

To further investigate the effect of synthesis conditions on PPO immobilization, the same two analyses described in the PEG-content study, entrapment efficiency and retention of enzymatic activity, were applied to microgels prepared at different synthesis pH values. This allowed us to evaluate how the pH during microgel formation influences enzyme incorporation and preservation of PPO catalytic activity. Result as shown in Table S2. At synthesis pH value below the pKa of the polymer, the microgel network remains collapsed a densely packed, limiting the enzyme diffusion into the inner regions of the matrix. As a result, only partial immobilization was achieved, and measurable PPO activity remained in the supernatant. At pH values of 7.0, the microgel becomes highly swollen and develops a high negative charge density. This pronounced electrostatic repulsion enzyme-polymer further reduced the immobilization efficiency, as evidenced by the elevated PPO activity detected in the supernatant (~38 %). In contrast, synthesis at pH 6 resulted in complete enzyme entrapment, with no detectable activity in the supernatant. This intermediate p, close to the pKa of pMAA, produces a partially swollen network with moderate charge density, minimizing excessive electrostatic repulsion while preserving sufficient conformational flexibility to retain PPO effectively. The percentage activity loss vs. free PPO reflects the extent to which the catalytic activity of the immobilized enzyme is reduced compared to that of the native, soluble PPO. Despite differences in immobilization efficiency across pH conditions, the activity loss of the immobilized PPO remained relatively low (15–20 %), demonstrating that the microgel network preserves PPO catalytic function to a significant extent once the enzyme is retained within the matrix.

3.3. Optimization of the biosensor working conditions

3.3.1. Effect of potential, pH and temperature

The biosensor response as a function of the applied potential was evaluated between −0.2 and 0.0 V in 0.05 M PBS (pH 6.0) containing 0.5 mM tyramine. The maximum amperometric response was observed in the range of −0.05 to −0.1 V. The current decreased slightly to higher potentials (≈35 % signal loss at 0 V) and more markedly at more negative potentials (≈60 % loss at −0.2 V), likely due to electrode fouling caused by the polymerization of enzymatically generated o-quinones [31]. To minimize potential interferences from other compounds, a potential as close as possible to zero was chosen, and −0.05 V was selected for all subsequent measurements.

The influence of pH on the biosensor response was investigated in the range of 4.5–8.0 using 0.5 mM tyramine in 0.05 M acetate/0.05 M phosphate buffer. A bell-shaped profile was observed, with the maximum response at pH 6.5 (Fig. 3). Increasing the pH by one unit from the optimum resulted in a 30 % decrease in current, while at pH 8.0 the signal dropped by nearly 60 %. Lowering the pH below the optimum caused an even more pronounced reduction in the amperometric response. The optimum value obtained is close to that reported for the free enzyme [32] and, as discussed in Section 3.4.3, corresponds to a pH at which the microgel is in a swollen state, facilitating substrate diffusion into the microparticles and the release of the enzymatic product. Therefore, all subsequent experiments were performed in PBS at pH 6.5.

The effect of temperature on the biosensor response was evaluated between 10 and 55 °C using 0.5 mM tyramine under oxygen-saturated conditions to avoid oxygen limitation. The current increased with temperature, reaching a maximum at 30 °C (Fig. 3), and then decreased at higher temperatures. To select an appropriate working temperature that prevents possible enzyme denaturation, thermal stability tests were conducted at 25 and 30 °C. A marked decrease in steady-state current at 30 °C is observed, indicated partial enzyme inactivation; therefore, 25 °C was chosen for all subsequent measurements. The Arrhenius plot for the enzyme immobilized in PEG–pMAA microparticles (η = 2.0 %)

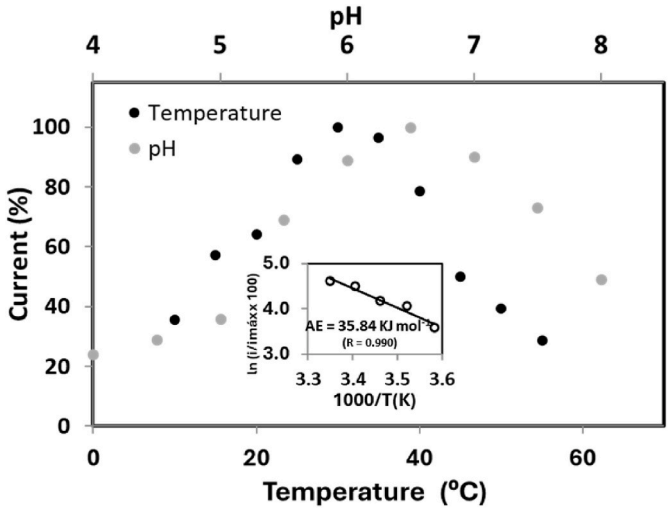

Fig. 3. Effect of pH and temperature on tyramine biosensor response based on PPO-PEG-pMAA, η = 2 %. The current is shown as normalized current (% I_{max}), with the highest measured value at 0.5 mM tyramine concentration set to 100 %. Inset: Arrhenius plot.

showed a single linear region, yielding an apparent activation energy of 35.84 kJ mol^{-1}—substantially higher than that of PPO in solution (1.85 kJ mol^{-1}) [33]. The single linear region suggests the absence of major conformational transitions within the studied temperature range and confirms that the immobilization matrix remained stable.

3.3.2. *Effect of the enzyme loading*

To optimize the performance of PPO-PEG–pMAA microgels and to extend the biosensor's application range, the influence of enzyme loading was examined from two perspectives: (i) variation of the amount of enzyme incorporated into the microgel during synthesis, and (ii) modification of the amount of microparticles deposited on the electrode surface. As shown in Table 2, both the sensitivity and the linear response range increased when the enzyme content in the microgel synthesis was raised from 2000 to 3000 U/mL, with no significant improvement observed at higher loadings. Taking this value as optimal, different amounts of microparticles were then deposited on the electrode surface.

Table 2
Analytical properties of PPO-PEG-pMAA biosensors as a function of enzyme loading.

PPO immobilized into the microparticles (U/mL)[a]	J_{max} (μA/cm^2)	Sensitivity (mA/Mcm^2)	Linear range (M)	R^2 (n)
2000	210.5	3.05×10^3	5.0×10^{-7} to 2.5×10^{-5}	0.987 (6)
3000	335.6	3.99×10^3	2.0×10^{-7} to 5.0×10^{-5}	0.991 (7)
4000	337.2	4.10×10^3	2.0×10^{-7} to 6.0×10^{-5}	0.994 (8)
Microparticles placed on the electrode (mg)[b]				
1	198.7	2.57×10^3	4.0×10^{-7} to 2.5×10^{-5}	0.991 (7)
2	335.6	3.99×10^3	2.0×10^{-7} to 5.0×10^{-5}	0.992 (7)
3	349.3	4.30×10^3	2.0×10^{-7} to 6.0×10^{-5}	0.987 (8)

[a] 2 mg.
[b] 3000 UI/mL.

The best analytical characteristics were obtained using 3 mg of microgels; however, this resulted in a notable increase in the response time (120 s for 3 mg vs. 50 s for 2 mg). Considering that 2 mg of microgels provided approximately 93 % of the sensitivity achieved with 3 mg, this value was selected as the optimum, representing a compromise between high detection capability for tyramine and a short analysis time.

To investigate how enzyme loading affects substrate and product diffusion, the redox behavior of a 5 mM $Fe(CN)_6^{3-}/Fe(CN)_6^{4-}$ solution was studied by electrochemical impedance spectroscopy (EIS). Fig. S1 shows the Nyquist plots of a bare GCE and a GCE modified with different amounts of PPO–PEG–pMAA microparticles (η = 2 %). As expected, increasing the microparticle coverage on the electrode surface led to higher charge transfer resistance (R_{ct} = 6780 Ω for 1 mg and R_{ct} = 11,570 Ω for 3 mg), reflecting the formation of a compact layer that hinders probe access. In contrast, variations in enzymatic loading within the microparticles had negligible effect on R_{ct} (approximately 7500 Ω in all cases, data not shown). These results indicate that, for a highly sensitive device, it is preferable to increase the amount of immobilized enzyme rather than the total microparticle coverage, as diffusion limitations arise primarily from excessive microparticle deposition.

3.4. *Biosensor behavior under optimal experimental conditions*

The performance of the biosensor for quantitative detection of tyramine was tested under optimal conditions (−0.1 V, pH 6, 25 °C, η = 2 %, 5 % PEG, 3000 UI/mL of PPO, 2 mg of microparticles). A linear relationship between the current signal and the tyramine concentration was obtained in the range $2.0 \bullet 10^{-7}$ to $4.7 \bullet 10^{-5}$ M (Fig. 4) with a regression equation of I (μA) = (279.19 ± 15.79) [Tyramine] (mM) + (0.097 ± 0.012), R = 0.9921 (n = 14). The detection and quantification limits were 4.5×10^{-8} and 1.2×10^{-7} M, respectively. The inset in Fig. 4 presents the complete calibration curve (top) and the time-dependent current response at different tyramine concentrations (bottom), demonstrating the rapid and reproducible response of the biosensor.

The apparent Michaelis–Menten constant ($K_{M,app}$) offers critical insight into the enzyme–substrate kinetics of biosensors. In the PEG–pMAA system, $K_{M,app}$ was determined to be 40 μM, based on a Lineweaver–Burk analysis (a value that is markedly lower than those typically reported for free/native PPO in solution). In several studies, PPO from different sources exhibits K_m values in the millimolar range. For example: in *Volvariella bombycina* PPO (catechol as substrate) Km = 1.67 mM [34]. In PPO from *Opuntia ficus*-indica, K_m values between 5.4 and 16.7 mM were reported depending on the diphenolic substrate used [35]. The substantially lower $K_{M,app}$ of the immobilized system implies

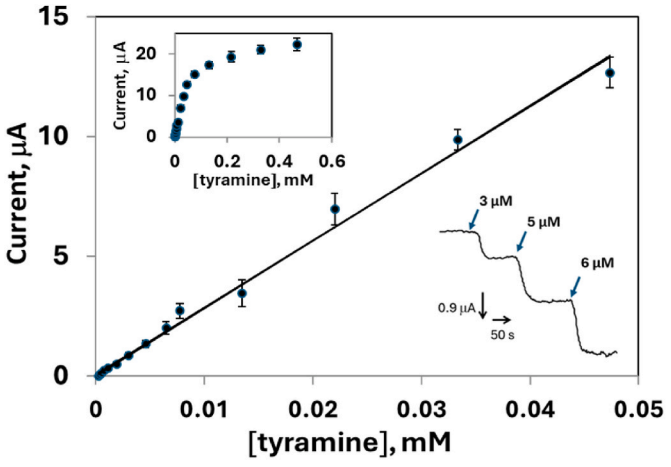

Fig. 4. Linear range of the calibration curve under optimal conditions. Inset: Complete calibration curve (top) and time-dependent current response to different concentrations of tyramine (bottom).

an enhanced affinity between PPO and tyramine, possibly due to favorable conformational constraints or improved substrate accessibility when PPO is immobilized in the microgel environment. In addition, a Hill coefficient of 1.2 is observed, that suggests slight positive cooperativity, which may reflect subtle enzyme-enzyme or enzyme-matrix interactions arising from immobilization. Together, these kinetics parameters demonstrate that the PEG–pMAA modified electrode combines high substrate affinity with a near-classical Michaelis–Menten behavior, yielding a sensitive, robust biosensing platform.

3.5. Biosensor precision and stability

The precision of the tyramine biosensor was evaluated under optimized conditions in terms of repeatability, intermediate precision, and reproducibility. Repeatability was assessed through 10 successive amperometric measurements at three tyramine concentrations (0.4, 4.0, and 40 μM) using the same biosensor. Intermediate precision was determined by repeating the procedure on five consecutive days with the same device, while reproducibility was evaluated using three independently fabricated biosensors, each tested in five replicates. As summarized in Table 3, all relative standard deviation (RSD) values were below 8.5 % and within the limits proposed by Horwitz [28] for the corresponding analyte concentrations, confirming the excellent precision of the PPO-PEG–pMAA microgel-based biosensor.

The stability of the system was evaluated from two complementary perspectives: the stability of the freeze-dried microparticles and the operational stability of the biosensor assembled with these materials. Regarding the biological component, the enzymatic activity of tyrosinase immobilized within the freeze-dried microgels remained unchanged for at least 9 months after synthesis, demonstrating the excellent preservation of the enzyme within the polymeric network. On the other hand, the stability of the biosensor was assessed by periodically recording the amperometry response toward tyramine, keeping the electrode stored in a phosphate buffer solution at −4 °C between measurements. The biosensor retained 95–100 % of its initial current response for 35 days, after which a marked decrease in signal intensity was observed. All results are shown in Fig. S2. When compared with biosensors employing other polymeric microparticle matrices for PPO immobilization, the system developed in this work demonstrates an improvement in operational stability. For example, a biosensor based on PPO immobilized within polyacrylamide microparticles retained activity for 27 days [28], biosensors based on poly(vinylimidazole) microparticles exhibited stability for only 10 days [36] and the use of poly ($ViEtIm^{+}Br^{-}$) microparticles in biosensor performance showed an operational lifetime of approximately 21 days [29]. These findings highlight that the PEG–pMAA microgel matrix offers a favorable microenvironment for enzyme stabilization and electron transfer, thereby extending the functional lifetime of the biorecognition layer.

The analytical performance of the proposed PEG-pMAA microgel-based biosensor was compared with previously reported tyrosinase electrochemical biosensors for tyramine determination. As summarized in Table 4, the developed biosensor exhibited the lowest detection limit compared with another immobilization matrices and close to the obtained by a biosensor prepared with brushite as inorganic matrix for enzyme immobilization [37]. This enhanced sensitivity can be attributed to the favorable microenvironment provided by the PEG-pMAA microgels, which promotes efficient enzyme activity and electron transfer. An additional advantage of the present approach lies in the simplicity of device fabrication. Once synthesized, the microgel particles remain stable under frozen conditions. Therefore, the preparation of the analytical bio platform involves only the deposition of the microparticles onto the electrode surface followed by securing with a dialysis membrane, allowing the biosensor to be ready for use in approximately 1 min. This combination of high analytical performance, stability, and ease of preparation makes the proposed system highly attractive for practical applications in food analysis and quality control. In addition, the PEG-pMAA microgel strategy is readily generalizable to other enzyme-based biosensors. In fact, pMAA microgels have previously been successfully used for the immobilization of glucose oxidase (GOx), demonstrating the versatility of this polymer network for different enzymes [16].

Table 3
Precision study of the PPO-PEG-pMAA biosensor.

Concentration assayed (μM)	Repeatability (CV, %)	Intermediate precision (CV, %)	Reproducibility (CV, %)
0.4	6.1	7.6	8.4
4	5.8	7.2	8.0
40	5.2	6.7	7.5

Table 4
Comparison of performances of different electrochemical tyrosinase biosensors for tyramine determination.

Immobilization system	Sensitivity (mA/Mcm^2)	Linear range (M)	Detection limit (M)	Ref.
Gold nanoparticle doped poly (8-anilino-1-naphthalene sulphonic acid)	1.90×10^{1}	1.0×10^{-5} to 1.2×10^{-4}	7.1×10^{-7}	[7]
Ionic liquid, carbon nanofiber and poly (glutamic acid)	2.41×10^{3}	2.0×10^{-7} to 4.8×10^{-5}	9.1×10^{-8}	[8]
Brushite and glutaraldehyde	15.0×10^{2}	5.8×10^{-7} to 1.6×10^{-5}	4.85×10^{-8}	[37]
Polymeric film derived from 4-mercaptophenylacetic acid (MPAA).	10^{3}	1.0×10^{-5} to 6.0×10^{-5}	3.16×10^{-6}	[38]
Carboxyl functionalized single-walled carbon nanotubes	59.0×10^{2}	5.0×10^{-6} to 1.8×10^{-4}	6.20×10^{-7}	[39]
Titania sol-gel modified with carbon materials and polymers	4.86×10^{2}	6.0×10^{-6} to 1.3×10^{-4}	1.5×10^{-6}	[40]
Adsorption in pencil hand-drawing electrode	5.08 mA/M	3.64×10^{-5} to 1.09×10^{-3}	2.92×10^{-6}	[41]
polyethylene glycol -p Methacrylic acid microgels	3.99×10^{3}	2.0×10^{-7} to 4.7×10^{-5}	4.5×10^{-8}	This work

3.6. Interference study

The selectivity of the tyrosinase-based biosensor for tyramine in cheese matrices was evaluated through an interference study. The most abundant inorganic acids and amino acids commonly present in fermented dairy products were tested at concentrations typical of these samples (Fig. 5). In addition, two biogenic amines, histamine and putrescine, were evaluated at concentrations typical of cheeses. In the presence of 40 μM tyramine, the amperometry responses of all potential interferents remained within ±3σ of the control measurements (n = 3, dashed lines in Fig. 5), demonstrating negligible interference. The no interferent (NI) condition is shown for reference. These results confirm the high selectivity of the biosensor, highlighting its suitability for accurate tyramine determination in complex food matrices.

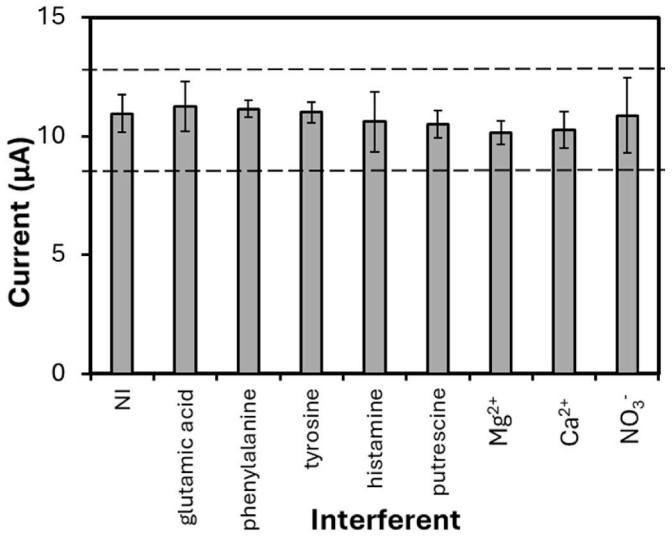

Fig. 5. Effects of 10 mM glutamic acid, 10 mM phenylalanine, 5 mM tyrosine, 1 mM histamine, 1 mM putrescine, 0.5 mM Mg^{2+}, 0.5 mM Ca^{2+}, and 0.5 mM NO_3^- on the response in the presence of 40 μM tyramine. Data for the NI (no interferent) condition is shown for reference, and the dashed lines represent ±3σ of the control measurements (n = 3).

3.7. Biosensor application in real samples

The accuracy of the proposed PPO–PEG–pMAA biosensor was initially validated through recovery studies in PBS at three different tyramine concentrations, yielding values consistently close to 100 % (Table 5), confirming both the precision and robustness of the method. The biosensor was then applied to real cheese samples, specifically Gouda and Brie, which were selected due to their fermented nature and propensity to accumulate biogenic amines, with tyramine being of particular concern [42]. Monitoring tyramine is critical not only because of its potential health risks, including hypertensive crises and migraines, but also as a sensitive indicator of product quality, reflecting microbial activity and storage or processing conditions [43]. After appropriate sample pretreatment, tyramine concentrations were quantified, and recovery studies yielded values ranging from 97.7 to 102.4 % for Brie, and from 97.6 to 105.6 % for Gouda cheese (Table 5). To evaluate the potential of the biosensor for monitoring cheese spoilage, a piece of Brie cheese was stored at room temperature for seven days, and the tyramine content was measured. As summarized in Table 3, tyramine levels increased over this period, reflecting the accumulation of biogenic amines under inadequate storage conditions. In a recovery study, a value of 102.7 % was obtained. These results demonstrate that the biosensor provides reliable and accurate measurements in complex food matrices, underscoring its potential as a rapid and practical tool for tyramine monitoring in dairy products.

Table 5
Analytical recovery in PBS and cheese samples.

Sample	Tyramine determinated (μM)	Tyramine added (μM)	Tyramine found (μM)[a]	Recovery (%)
PBS	–	1	1.04 ± 0.12	104.0
	–	2	2.11 ± 0.25	105.5
	–	5	4.82 ± 0.58	96.4
Brie cheese	1.2	1	2.15 ± 0.21	97.7
	1.2	2	3.26 ± 0.27	101.9
	1.2	5	6.35 ± 0.54	102.4
Gouda cheese	4.3	1	5.24 ± 0.42	104.8
	4.3	2	6.15 ± 0.65	97.6
	4.3	5	9.82 ± 0.85	105.6
Brie chesse[a]	4.7	5	9.97 ± 0.85	102.7

**7 days of storage at room temperature before measurement.
[a] Values are given as mean value ± SD (n = 5).

The PEG–pMAA microgel-based biosensor presents significant potential for miniaturization into a disposable point-of-care platform, enabling rapid and on-site screening of tyramine in diverse food matrices. Its stable enzyme immobilization, fast amperometric response, and compatibility with small-scale electrode formats make it a promising candidate for practical applications in food safety monitoring. While the biosensor demonstrated excellent performance in cheese samples, potential limitations should be considered for broader application in complex food matrices. High levels of fats, proteins, or polysaccharides may adsorb onto the sensor surface, partially obstructing enzyme accessibility or hindering substrate and product diffusion. Moreover, variations in pH, ionic strength, or the presence of antioxidants and preservatives in different matrices could affect tyrosinase activity or electron transfer efficiency. Additionally, other biogenic amines not evaluated in this study, such as cadaverine, spermidine, and spermine, may coexist in certain foods and potentially interfere with the sensor response. These factors should be carefully considered when extending the use of the PEG–pMAA microgel-based biosensor to diverse food products, and appropriate sample preparation or matrix-correction strategies may be required to ensure accurate and reliable tyramine quantification.

4. Conclusions

In this work, a highly sensitive and selective electrochemical biosensor for tyramine detection was developed by immobilizing tyrosinase within polyethylene glycol-poly(methacrylic acid) microgels (PEG-pMAA). The incorporation of PEG in the polymerization process enhanced the electrochemical response by 22 % compared to PEG-free microgels, likely due to a more favorable microenvironment for enzyme activity, without compromising reproducibility (RSD ≤6.1 %). Under optimized conditions, the biosensor exhibited a wide linear range (2.0×10^{-7} – 4.7×10^{-5} M), excellent sensitivity (3.99×10^3 mA/Mcm^2), and low detection limit (LOD = 4.5×10^{-8} M). The freeze-dried microgels remained unchanged for at least 9 months after synthesis, demonstrating the excellent preservation of the enzyme within the polymeric network. The PEG-pMAA microgel-based biosensor maintained 95–100 % of the amperometry response to tyramine over 35 days, demonstrating robust operational stability. Recovery studies in PBS and Brie cheeses confirmed the accuracy and robustness of the method, with values close to 100 %, while interference studies verified the selectivity of the biosensor toward tyramine in the presence of potential interfering compounds. Overall, the results demonstrate that the PPO-PEG-pMAA microgel-based biosensor provides a fast, accurate, and reproducible platform for tyramine determination in complex food matrices. Its high sensitivity, excellent stability, and reliable performance highlight its potential as a practical tool for monitoring biogenic amines in dairy products, contributing both to food safety and quality assessment.

CRediT authorship contribution statement

Juan Pablo Hervás-Pérez: Writing – review & editing, Writing – original draft, Supervision, Investigation, Data curation. **Laura Martín-Carbajo:** Writing – review & editing, Writing – original draft, Investigation, Data curation. **Sergio Izcara:** Writing – review & editing, Writing – original draft, Investigation, Formal analysis. **Marta Sánchez-Paniagua:** Writing – review & editing, Writing – original draft, Visualization, Supervision, Investigation, Formal analysis, Data curation, Conceptualization.

Declaration of competing interest

The authors declare that they have no known competing financial interests or personal relationships that could have appeared to influence

the work reported in this paper.

Acknowledgements

The authors gratefully acknowledge the support of the Research Group 921114 – Plant-Based Foods: Processing, Quality and Functional Ingredients, Complutense University of Madrid, for their valuable guidance and access to resources. The funding was provided through the direct award call for Research Groups at the Complutense University of Madrid (UCM), reference GRFN24/24.

Appendix A. Supplementary data

Supplementary data to this article can be found online at https://doi.org/10.1016/j.talanta.2025.129253.

Data availability

Data will be made available on request.

References

[1] N. Saha Turna, R. Chung, L. McIntyre, A review of biogenic amines in fermented foods: occurrence and health effects, Heliyon 10 (2024) e24501, https://doi.org/10.1016/J.HELIYON.2024.E24501.
[2] G. Natrella, M. Vacca, F. Minervini, M. Faccia, M. De Angelis, A comprehensive review on the biogenic amines in cheeses: their origin, chemical characteristics, hazard and reduction strategies, Foods 13 (2024) 2583, https://doi.org/10.3390/FOODS13162583/S1.
[3] B. del Rio, M. Fernandez, B. Redruello, V. Ladero, M.A. Alvarez, New insights into the toxicological effects of dietary biogenic amines, Food Chem. 435 (2024) 137558, https://doi.org/10.1016/J.FOODCHEM.2023.137558.
[4] A. Önal, S.E.K. Tekkeli, C. Önal, A review of the liquid chromatographic methods for the determination of biogenic amines in foods, Food Chem. 138 (2013) 509–515, https://doi.org/10.1016/J.FOODCHEM.2012.10.056.
[5] M.A. Munir, K.H. Badri, L.Y. Heng, S. Ibrahim, Biogenic amines detection by chromatography and sensor methods: a comparative review, Science and Technology Indonesia 5 (2020) 90–110, https://doi.org/10.26554/STI.2020.5.4.90-110.
[6] S. Kashyap, N. Tehri, N. Verma, A. Gahlaut, V. Hooda, Recent advances in development of electrochemical biosensors for the detection of biogenic amines, 3 Biotech 13 (1) (2022) 1–15, https://doi.org/10.1007/S13205-022-03414-W, 13 (2022).
[7] W. da Silva, M.E. Ghica, R.F. Ajayi, E.I. Iwuoha, C.M.A. Brett, Tyrosinase based amperometric biosensor for determination of tyramine in fermented food and beverages with gold nanoparticle doped poly(8-anilino-1-naphthalene sulphonic acid) modified electrode, Food Chem. 282 (2019) 18–26, https://doi.org/10.1016/J.FOODCHEM.2018.12.104.
[8] İ. Okman Koçoğlu, P.E. Erden, E. Kılıç, Disposable biosensor based on ionic liquid, carbon nanofiber and poly(glutamic acid) for tyramine determination, Anal. Biochem. 684 (2024), https://doi.org/10.1016/J.AB.2023.115387.
[9] A.V. Bounegru, C. Apetrei, Tyrosinase immobilization strategies for the development of electrochemical Biosensors—A review, Nanomaterials 13 (2023) 760, https://doi.org/10.3390/NANO13040760. Page 760 13 (2023).
[10] G. Sun, X. Wei, D. Zhang, L. Huang, H. Liu, H. Fang, Immobilization of enzyme electrochemical biosensors and their application to food bioprocess monitoring, Biosensors 13 (2023) 886, https://doi.org/10.3390/BIOS13090886. Page 886 13 (2023).
[11] M. Chen, G. Bolognesi, G.T. Vladisavljević, Crosslinking strategies for the microfluidic production of microgels, Molecules 26 (2021) 3752, https://doi.org/10.3390/MOLECULES26123752. Page 3752 26 (2021).
[12] A.T. Silva, R. Figueiredo, M. Azenha, P.A.S. Jorge, C.M. Pereira, J.A. Ribeiro, Imprinted hydrogel nanoparticles for protein biosensing: a review, ACS Sens. 8 (2023) 2898–2920, https://doi.org/10.1021/ACSSENSORS.3C01010/ASSET/IMAGES/LARGE/SE3C01010_0013.JPEG.
[13] X. Huang, J. Li, Y. Araki, T. Wada, Y. Xu, M. Takai, Enzyme stability in polymer hydrogel–enzyme hybrid nanocarrier containing phosphorylcholine group, RSC Adv. 14 (2024) 18807–18814, https://doi.org/10.1039/D4RA02436B.
[14] M. Hu, Y. Tang, X. He, K. Liu, L. Qin, X. Wang, Q. Wang, Enzyme-Integrated hydrogels for advanced biological applications, Polymer Science & Technology (2025), https://doi.org/10.1021/POLYMSCITECH.5C00076.
[15] Y. Wen, X. Wang, J. Zhao, X. Zhai, W. Xia, P. Li, K. Lai, L. Wu, Preparation and application of enzyme-based hydrogels, Biosens. Bioelectron. X 23 (2025) 100594, https://doi.org/10.1016/J.BIOSX.2025.100594.
[16] J.P. Hervás Pérez, B. López-Ruiz, E. López-Cabarcos, Synthesis and characterization of microparticles based on poly-methacrylic acid with glucose oxidase for biosensor applications, Talanta 149 (2016) 310–318, https://doi.org/10.1016/J.TALANTA.2015.11.053.
[17] Y.R. Maghraby, R.M. El-Shabasy, A.H. Ibrahim, H.M.E.S. Azzazy, Enzyme immobilization technologies and industrial applications, ACS Omega 8 (2023) 5184, https://doi.org/10.1021/ACSOMEGA.2C07560.
[18] K. Sakdaphetsiri, S. Teanphonkrang, A. Schulte, Cheap and sustainable biosensor fabrication by enzyme immobilization in commercial polyacrylic Acid/Carbon nanotube films, ACS Omega 7 (2022) 19347–19354, https://doi.org/10.1021/ACSOMEGA.2C00925.
[19] U. Hwang, H.Y. Moon, J. Park, H.W. Jung, Crosslinking and swelling properties of pH-Responsive Poly(Ethylene Glycol)/Poly(Acrylic acid) interpenetrating polymer network hydrogels, Polymers 16 (2024) 2149, https://doi.org/10.3390/POLYM16152149. Page 2149 16 (2024).
[20] A. Wozniak, V. Humblot, R. Vayron, R. Delille, C. Falentin-Daudré, Simple UV-Grafting of PolyAcrylic and PolyMethacrylic acid on silicone breast implant surfaces: Chemical and mechanical characterizations, Coatings 13 (2023) 1888, https://doi.org/10.3390/COATINGS13111888. Page 1888 13 (2023).
[21] Z. Wang, Q. Ye, S. Yu, B. Akhavan, Poly ethylene glycol (PEG)-Based hydrogels for drug delivery in cancer therapy: a comprehensive review, Adv. Healthcare Mater. 12 (2023), https://doi.org/10.1002/ADHM.202300105.
[22] G.J. Rodriguez-Rivera, M. Green, V. Shah, K. Leyendecker, E. Cosgriff-Hernandez, A user's guide to degradation testing of polyethylene glycol-based hydrogels: from in vitro to in vivo studies, J. Biomed. Mater. Res. 112 (2024) 1200–1212, https://doi.org/10.1002/JBM.A.37609.
[23] Y. Liu, H. Hou, Y. Zhang, Y. Zheng, M. Sun, H. Yuan, T. Guo, T. Meng, Polyethylene glycol-enzyme nanocomplexes as carrier-free biocatalyst for pickering interfacial catalysis, ACS Appl. Bio Mater. 7 (2024) 7023–7029, https://doi.org/10.1021/ACSABM.4C01186/ASSET/IMAGES/LARGE/MT4C01186_0004.JPEG.
[24] Q. Xu, J. Hou, J. Rao, G.H. Li, Y.L. Liu, J. Zhou, PEG modification enhances the in vivo stability of bioactive proteins immobilized on magnetic nanoparticles, Biotechnol. Lett. 42 (2020) 1407–1418, https://doi.org/10.1007/S10529-020-02867-4/FIGURES/3.
[25] J.P.H. Pérez, E. López-Cabarcos, B. López-Ruiz, Amperometric glucose biosensor based on biocompatible poly(dimethylaminoethyl) methacrylate microparticles, Talanta 81 (2010) 1197–1202, https://doi.org/10.1016/J.TALANTA.2010.02.010.
[26] J.P. Hervás Pérez, E. López-Cabarcos, B. López-Ruiz, Encapsulation of glucose oxidase within poly(ethylene glycol) methyl ether methacrylate microparticles for developing an amperometric glucose biosensor, Talanta 75 (2008) 1151–1157, https://doi.org/10.1016/J.TALANTA.2008.01.030.
[27] K. Sannohe, T. Ma, S. Hayase, Synthesis of monodispersed silver particles: synthetic techniques to control shapes, particle size distribution and lightness of silver particles, Adv. Powder Technol. 30 (2019) 3088–3098, https://doi.org/10.1016/J.APT.2019.09.015.
[28] J.P. Hervás Pérez, M. Sánchez-Paniagua López, E. López-Cabarcos, B. López-Ruiz, Amperometric tyrosinase biosensor based on polyacrylamide microgels, Biosens. Bioelectron. 22 (2006) 429–439, https://doi.org/10.1016/J.BIOS.2006.05.015.
[29] M. Sánchez-Paniagua López, B. López-Ruiz, Electrochemical biosensor based on ionic liquid polymeric microparticles. An analytical platform for catechol, Microchem. J. 138 (2018) 173–179, https://doi.org/10.1016/J.MICROC.2018.01.011.
[30] S. Bhattacharjee, S. Goswami, S. Das, S. Bhattacharjee, S. Bhaladhare, pH-responsive, stable, and biocompatible functional nanogels based on chitosan (CS)/poly methacrylic acid (PMAA) polymers: synthesis and characterization, Mater. Today Commun. 36 (2023) 106541, https://doi.org/10.1016/J.MTCOMM.2023.106541.
[31] F. Liu, A.J. Reviejo, J.M. Pingarrón, J. Wang, Development of an amperometric biosensor for the determination of phenolic compounds in reversed micelles, Talanta 41 (1994) 455–459, https://doi.org/10.1016/0039-9140(94)80152-5.
[32] R.S. Brown, K.B. Male, J.H.T. Luong, A substrate recycling assay for phenolic compounds using tyrosinase and NADH, Anal. Biochem. 222 (1994) 131–139, https://doi.org/10.1006/ABIO.1994.1464.
[33] K. Ikehata, J.A. Nicell, Characterization of tyrosinase for the treatment of aqueous phenols, Bioresour. Technol. 74 (2000) 191–199, https://doi.org/10.1016/S0960-8524(00)00025-0.
[34] A. Sarsenova, D. Demir, K. Çağlayan, S. Abiyev, T. Darbayeva, C. Eken, Purification and properties of polyphenol oxidase of dried Volvariella bombycina, Biology 12 (2023) 53, https://doi.org/10.3390/BIOLOGY12010053. Page 53 12 (2022).
[35] D. Demir, S. Kabak, K. Çağlayan, Purification and characterization of polyphenol oxidase in the fruits of Opuntia ficus-indica, Biology 12 (2023) 1339, https://doi.org/10.3390/BIOLOGY12101339. Page 1339 12 (2023).
[36] M.S.P. López, E. López-Cabarcos, B. López Ruiz, Biosensors based on Poly (vinylimidazole) microparticles, Electroanalysis 21 (2009) 512–520, https://doi.org/10.1002/ELAN.200804436.
[37] M. Sánchez-Paniagua López, E. Redondo-Gómez, B. López-Ruiz, Electrochemical enzyme biosensors based on calcium phosphate materials for tyramine detection in food samples, Talanta 175 (2017) 209–216, https://doi.org/10.1016/J.TALANTA.2017.07.033.
[38] I.P. Soares, A.G. da Silva, R. da Fonseca Alves, R.A.M. de Souza Corrêa, L. F. Ferreira, D.L. Franco, Electrochemical enzymatic biosensor for tyramine based on polymeric matrix derived from 4-mercaptophenylacetic acid, J. Solid State Electrochem. 23 (2019) 985–995, https://doi.org/10.1007/S10008-019-04204-W/TABLES/2.
[39] I.M. Apetrei, C. Apetrei, The biocomposite screen-printed biosensor based on immobilization of tyrosinase onto the carboxyl functionalised carbon nanotube for assaying tyramine in fish products, J. Food Eng. 149 (2015) 1–8, https://doi.org/10.1016/J.JFOODENG.2014.09.036.
[40] J. Kochana, K. Wapiennik, P. Knihnicki, A. Pollap, P. Janus, M. Oszajca, P. Kuśtrowski, Mesoporous carbon-containing voltammetric biosensor for

determination of tyramine in food products, Anal. Bioanal. Chem. 408 (2016) 5199–5210, https://doi.org/10.1007/S00216-016-9612-Y/TABLES/3.
[41] R. Torre, M. Cerrato-Alvarez, H.P.A. Nouws, C. Delerue-Matos, M.T. Fernández-Abedul, E. Costa-Rama, A hand-drawn graphite electrode for affordable analysis: application to the enzymatic determination of tyramine in fish, Sensor. Actuator. B Chem. 423 (2025) 136705, https://doi.org/10.1016/J.SNB.2024.136705.
[42] E. Dadáková, M. Křížek, T. Pelikánová, Determination of biogenic amines in foods using ultra-performance liquid chromatography (UPLC), Food Chem. 116 (2009) 365–370, https://doi.org/10.1016/J.FOODCHEM.2009.02.018.
[43] C. Ruiz-Capillas, F. Jiménez-Colmenero, Biogenic amines in meat and meat products, Crit. Rev. Food Sci. Nutr. 44 (2004) 489–599, https://doi.org/10.1080/10408690490489341.